2016

Laboratory Performance Evaluation Of Residential Scale Gas Engine Driven Heat Pump

Ahmad Abu-Heiba
Oak Ridge Associated Universities, United States of America, abuheibaag@ornl.gov

Isaac Y. Mahderekal
IntelliChoice Energy, imahderekal@iceghp.com

Ayyoub Momen
Oak Ridge National Laboratory, momena@ornl.gov

Laboratory Performance Evaluation of Residential Scale Gas Engine Driven Heat Pump

Ahmad Abu-Heiba[1]*, Isaac Mahderekal[2], Ayyoub Momen[1]

[1]Oak Ridge National Laboratory,
Oak Ridge, TN, USA
Phone: 1-865-576-6053

[2]IntelliChoice Energy,
Las Vegas, NV, USA
Phone: 1-702-815-0600

* Corresponding Author

ABSTRACT

Building space cooling is, and until 2040 is expected to continue to be, the single largest use of electricity in the residential sector in the United States. Increases in electric-grid peak demand leads to higher electricity prices, system inefficiencies, power quality problems, and even failures. Thermally-activated systems, such as gas engine-driven heat pumps (GHP), can reduce peak demand. This study describes the performance of a residential scale GHP. It was developed as part of a cooperative research and development agreement (CRADA) between Oak Ridge National Laboratory (ORNL) and Southwest Gas. Results showed the GHP produced 16.5 kW (4.7 RT) of cooling capacity at the 35°C (95°F) rating condition with a gas-based coefficient of performance (COP) of 0.99. In heating, the GHP produced 20.2 kW (5.75 RT) with a gas COP of 1.33. The study also discusses other benefits and challenges facing the GHP technology such as cost, reliability, and noise.

1. INTRODUCTION

A gas engine-driven heat pump (GHP) is a vapor compression cycle heat pump where a natural-gas-driven engine replaces an electric motor to drive the compressor. GHPs have several advantages over their conventional single-speed electric motor-driven counterparts. One very significant advantage is the variable-speed control of its output. Reducing capacity by slowing the engine maintains a high coefficient of performance (COP) during part load operation. Another advantage of the GHPs over their electric counterparts is their ability to use the heat rejected from the engine. The recovered heat is used to supplement the vapor compression cycle during heating. This increases the COP and enables the heat pump to operate at lower ambient temperatures than electric counterparts. The rejected heat may also be used to supply other process loads, such as water heating.

A report published by the United Kingdom Department of Energy and Climate Change (2014) estimated that more than 800,000 GHP units were installed in Asia. This high level of market penetration is attributed mainly to the peak demand reduction resulting from using GHP instead of electric counterparts especially where demand charges are high such as in Japan. Although it focused mainly on the European market, the barriers, opportunities and cost reduction potentials identified in the report are universal and provide useful insight to GHP developers globally. Sohn *et al.* (2008) reported on a year-long field-testing of six 10-ton GHPs at six United States Department of Defense installations in the south west region. The report presented the economic impact, reliability, and estimated environmental impact of the installed GHPs. Electric and gas utility combined cost net saving was reported for all installations. The savings ranged from $680 to $2,134. In 2012, a report released by the Building Technologies Office of the US Department of Energy estimated the energy saving potential of GHP technology in the residential sector to be 44 Terawatt-hour (0.15 Quads/year.)

Mahderekal *et al.* (2008) presented the design and development of a 10-ton GHP. The paper demonstrated the design challenges that had to be overcome and presented the results of laboratory performance evaluation. The main design challenges were focused on reducing cost, reducing the frequency of periodic maintenance, and complying with emissions regulations. The payback of their final design was estimated to be between 2 to 5 years based on natural gas and electricity prices in southern Nevada and Arizona. Mahderekal *et al.* (2012) modeled a 10-ton GHP with performance improvements. The paper reported a modeled 25% improvement in heating efficiency when engine waste heat is recovered in the suction line refrigerant heat exchanger. The model also included a desiccant wheel integrated to the GHP to augment dehumidification during cooling. The desiccant was regenerated by waste heat from the engine. The model estimated that using the desiccant system can lower the sensible heat ratio to 40%. Shen *et al.* (2013) modeled two GHP configurations; first with suction line refrigerant to coolant heat exchanger and second with the addition of supply air to coolant heating coil. The two configurations were simulated in EnergyPlus and the energy performance was compared to a baseline unit in 16 different US cities in different climate zones.. The baseline unit had electrically-driven air conditioner with seasonal COP of 4.1 for space cooling and a gas furnace with 90% fuel efficiency for heating.

In this paper, the performance of a residential scale GHP developed as part of a cooperative research and development agreement (CRADA) between Oak Ridge National Laboratory (ORNL) and Southwest Gas, has been comprehensively investigated.

2. GHP PROTOTYPE SPECIFICATIONS

The development of the GHP started in 2011 and the final commercialized prototype was built and tested in 2015. The developed GHP is a split air-source 4.5-ton heat pump that uses R410-A as the refrigerant. It uses a water-cooled, 4-stroke, single-cylinder, 270 cc, 5.6 kW (7.5 HP) engine. The engine is designed to run for 4,000 continuous hours before maintenance with 40,000 hour life expectancy before a major overhaul. The compressor is a scroll type with volumetric capacity of 60.5 cc/rev. The compressor is belt-driven by the engine. The outdoor fan motor is 1/3 horsepower. A two-stage indoor air handler was used. Figure 1 shows a piping and instrumentation diagram of the GHP.

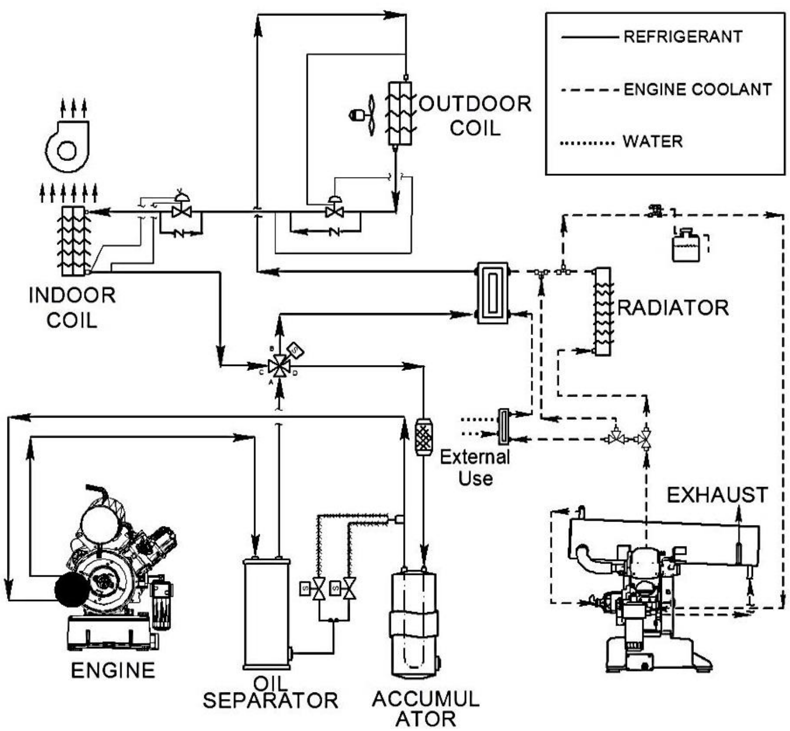

Figure 1. GHP schematic; space cooling mode operation shown.

The engine coolant circuit is equipped with two diverting valves. The first one is at the outlet of the coolant from the engine block. When the engine is cold, the valve diverts all coolant flow to a bypass path, where no heat is extracted from the coolant. This helps increase the engine temperature to its desired operating temperature. When the engine temperature reaches the desired operating temperature, the valve diverts the flow to the second diverting valve. When the coolant temperature is below its set point, the second diverting valve diverts all coolant flow to a refrigerant-to-coolant heat exchanger. When the coolant temperature exceeds the set point of the valve, it diverts all coolant flow to a domestic water-to-coolant heat exchanger, if it exists, then to the radiator. The radiator fan is activated by a temperature switch that senses the coolant temperature. During cooling operation, the hot refrigerant from the compressor flows through the refrigerant-to-coolant heat exchanger. Since it is hot, it does not remove enough heat from the coolant. The second diverting valve directs all flow to the domestic hot water heat exchanger, if it exists, then to the radiator. During heating operation, the cold refrigerant from the outdoor coil flows through the refrigerant-to-coolant heat exchanger. It gains heat from the coolant. Thus, it boosts the heating capacity of the GHP. This study describes and presents the laboratory performance evaluation of the GHP.

3. EXPERIMENT

Evaluation of the developed GHP was conducted in an environmental chamber at ORNL. The chamber consists of two rooms; outdoor and indoor. The outdoor (condensing) unit of the GHP was installed in the outdoor room while the air handler was installed in the indoor room. The unit was then operated over a wide range of ambient conditions and all data points needed to calculate capacity and COP were measured and recorded. Table 1 lists these conditions. The evaluations were conducted at high (3400 rpm), intermediate (2400 rpm), and low (1800 rpm) engine speeds.

Table 1. Operating conditions for evaluation of GHP.

	Air Entering					
	Indoor Unit			**Outdoor Unit**		
	Dry Bulb °C (°F)	**Dew Point °C (°F)**	**Wet Bulb °C (°F)**	**Dry Bulb °C (°F)**	**Dew Point °C (°F)**	**Wet Bulb °C (°F)**
Cooling	26.7 (80)	15.7 (60.2)	19.4 (67)	23.9 (75)	8.7 (47.7)	15 (59)[a]
	26.7 (80)	15.7 (60.2)	19.4 (67)	29.4 (85)	14.1 (57.4)	19.4 (67)[a]
	26.7 (80)	15.7 (60.2)	19.4 (67)	35 (95)	19.2 (66.5)	23.9 (75)[a]
	26.7 (80)	15.7 (60.2)	19.4 (67)	40.6 (105)	16.6 (61.8)	23.9 (75)[a]
	26.7 (80)	15.7 (60.2)	19.4 (67)	46.1 (115)	12.8 (55)	23.9 (75)[a]
	26.7 (80)	15.7 (60.2)	19.4 (67)	51.7 (125)	8.4 (47.1)	23.9 (75)[a]
Heating	21.1 (70)	11.9 (53.5)	15.6 (60) (max)	-8.3 (17)	-12.6 (9.4)	-9.4 (15)
	21.1 (70)	11.9 (53.5)	15.6 (60) (max)	1.7 (35)	-2 (28.4)	0 (32)
	21.1 (70)	11.9 (53.5)	15.6 (60) (max)	8.3 (47)	3.7 (38.7)	6.1 (43)
	21.1 (70)	11.9 (53.5)	15.6 (60) (max)	12.8 (55)	7.9 (46.2)	10.1 (50.2)
	21.1 (70)	11.9 (53.5)	15.6 (60) (max)	18.3 (65)	12 (53.6)	14.5 (58.1)

[a] Wet bulb condition is not required.

To reduce the noise on the measurement, the natural gas consumption was measured by a diaphragm type gas meter with pulse output. The refrigerant flow rate was measured by a Coriolis mass flow meter. Humidity transmitters were used to measure relative humidity. Supply air flow rates were measured using a multi-point, self-averaging Pitot traverse station with an integral air straightener/equalizer honeycomb cell. This arrangement allows the capability of continuously measuring fan discharges or ducted airflow. Thermocouples, tachometer, hygrometers and pressure transducers along with the flow rates measuring devices were used to monitor the GHP via a PC-based data acquisition system. Sensors for these measurements and their accuracies are shown in Table 2. The required accuracy of the test instrumentation is in accordance with ASHRAE and/or ASME documents (ASHRAE 2006; ASME 2004a, 2004b; ASHRAE 1989a.).

The air handler was operated on high-stage when in heating mode. In cooling mode the air handler was operated on low-stage when running the engine at low- and intermediate-speed (1800 and 2400 rpm respectively) and it was operated on high-stage when running the engine at high-speed (3400 rpm.)

Table 2. Test instrument and measurement accuracies.

Measurement	**Sensor**	**Range**	**Accuracy**
Temperature	T-Type Thermocouple	-270 to 400 °C (-454 to 752 °F)	±1 °C (±1.8 °F)
Pressure	Transducer	0 to 4,137 kPa (0 to 600 psia)	±1% of full scale
Air flow	Pitot tube array	0 to 2.08 m^3/s (0 to 4,400 cfm)	±2%
Natural gas flow	Diaphragm meter	0 to 0.001966 m^3/s (0 to 1.167 cfm)	±1%
Refrigerant flow	Coriolis mass flow sensor	0 to 15.12 kg/s (0 to 2,000 lb/hr)	±0.1%
Relative Humidity	Hygrometer	0 to 100 %RH	±2%RH
Engine speed	Tachometer	0 to 5,000 rpm	±0.1%
Electric power	Watt transducer	0 to 1,000 Watt	±0.5% of full scale

The airside capacity is calculated using the method outlined in 2005 ASHRAE Handbook of Fundamentals. The capacity is calculated by determining the saturation pressure of water vapor in the return or supply air, using the following equation and constants:

$$\ln p_{ws} = C_1/T + C_2 + C_3\,T + C_4\,T^2 + C_5\,T^3 + C_6\,\ln T \tag{1}$$

Where
$C_1 = -5.800\,220\,6$ E+03
$C_2 = 1.391\,499\,3$ E+00
$C_3 = -4.864\,023\,9$ E−02
$C_4 = 4.176\,476\,8$ E−05
$C_5 = -1.445\,209\,3$ E−08
$C_6 = 6.545\,967\,3$ E+00

The humidity ratio of the return or supply air is then obtained by using the following equation:

$$W = 0.6218\,\frac{p_{ws}}{p - p_{ws}} \tag{2}$$

The moist air specific enthalpy is then calculated as:

$$h = 1.006\,t + W\,(2501 + 1.805\,t) \tag{3}$$

After the enthalpy is obtained for both the return and supply air, the specific volume of dry air is calculated with the following equation:

$$v = 0.2871\,\,(t + 273.15)(1 + 1.6078\,W)/P \tag{4}$$

Using the above equation, the density of moist air becomes:

$$\rho = (1/v)(1 + W) \tag{5}$$

The mass flow rate of air is then calculated as:

$$\dot{m} = \rho\,\dot{V} \tag{6}$$

Finally, the total airside capacity is calculated by determining the difference between the return and the supply air enthalpies and multiplying it by the mass flow rate of the moist air:

$$\dot{Q}_T = \dot{m}\,(h_r - h_s) \tag{7}$$

The sensible and latent capacities are given by the following equations:

$$\dot{Q}_S = \dot{m}\,\,C_p\,(T_r - T_s) \tag{8}$$

$$\dot{Q}_L = \dot{Q}_T - \dot{Q}_S \tag{9}$$

The sensible heat ratio is calculated as:

$$SHR = \frac{\dot{Q}_{Sensible}}{\dot{Q}_{Total}} \tag{10}$$

In this paper, the coefficient of performance (COP) is the Gas-COP, and is calculated as:

$$COP = \frac{\dot{Q}_{Total}}{Fuel\ Input} \tag{11}$$

4. RESULTS

Evaluation of the GHP unit in heating mode was completed over a wide range of conditions (engine speeds, outdoor and indoor temperatures, and humidity). Figure 2 and Figure 3 show the performance at high, intermediate and low engine speeds. Gas heating COP of 1.33 with capacity of 20.2 kW (69,000 Btu/h or 5.75 RT) at AHRI steady-state rating condition of 8.3°C (47°F) outdoor was achieved at high engine speed.

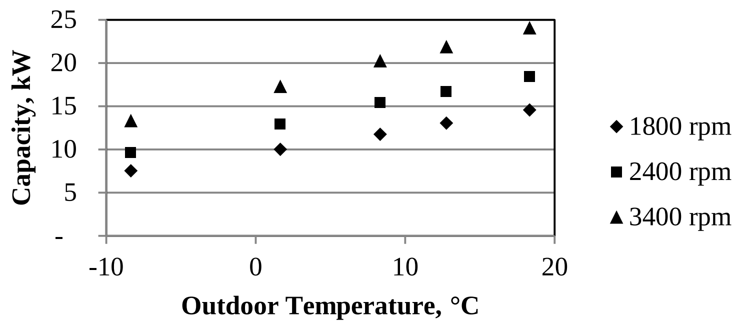

Figure 2. Heating capacity of the GHP at three different speeds.

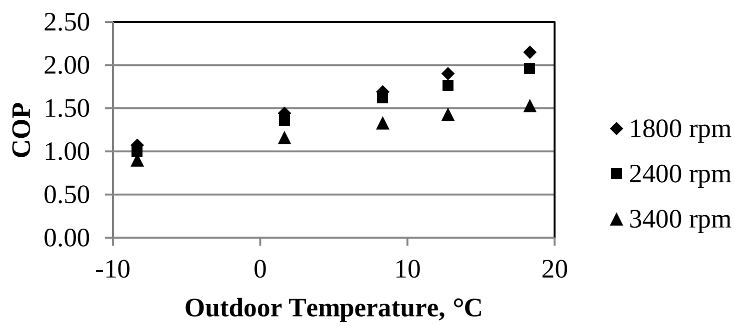

Figure 3. Heating coefficient of performance of the GHP.

Evaluation of the GHP unit in cooling mode was completed over a wide range of conditions (engine speeds, outdoor and indoor temperatures, and humidity). Figure 4 and Figure 5 show the cooling performance at high, intermediate and low engine speeds. As shown in Figure 4 and Figure 5, gas cooling Coefficient of Performance (COP) of 0.99 at AHRI steady-state rating condition of 35°C (95°F) outdoor and 26.7°C (80°F) dry-bulb/15.7°C (60.2°F) dew-point temperatures for indoor with capacity of 15.8 kW (53,965 Btu/h or 4.5 RT) was achieved at high engine speed.

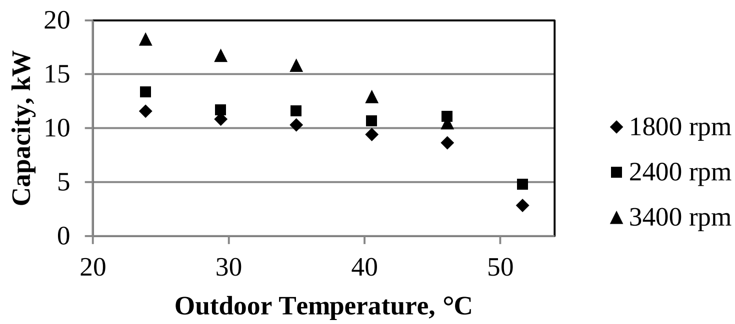

Figure 4. Cooling capacity of the GHP at three different speeds.

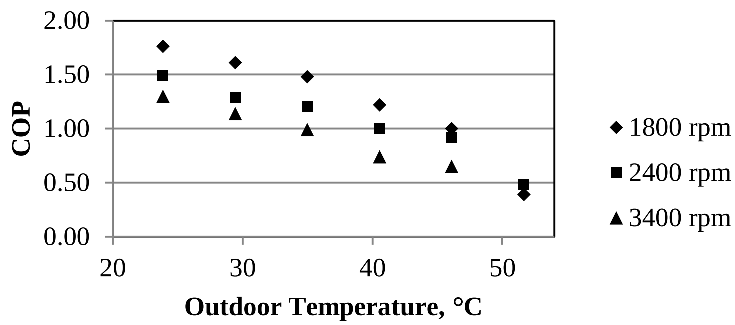

Figure 5. Cooling coefficient of performance of the GHP.

The GHP unit was not tested at 51.7°C (125°F) outdoor temperature and 3400 rpm. At that condition, the engine did not have enough output power to overcome the load resulting from the high discharge pressure and stalled. Similarly, at 2400 and 1800 rpm and 51.7°C (125°F) outdoor temperature, the engine did not run at exactly those speeds. It rather ran at 2200 and 1650 rpm respectively. This explains the steep drop in cooling capacity seen in Figure 4 at 51.7°C (125°F) outdoor temperature.

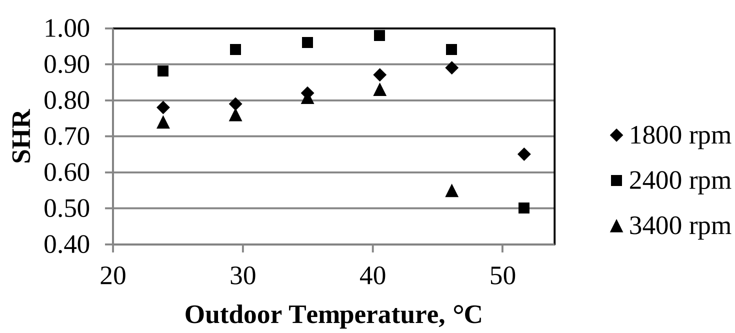

Figure 6. Sensible Heat ratio in cooling mode at different speeds.

As shown in Figure 4, the intermediate speed cooling capacity is less than would be expected. It's only slightly higher than it is at low speed and significantly less than it is at high speed. This is attributed to the high sensible heat ratio, or low latent cooling capacity, at intermediate speed. Sensible heat ratio for all test condition is shown in Figure 6. The high sensible heat ratio at intermediate speed was the result of running the air handler on high speed.

Electric condenser fan power consumption of the GHP varies slightly with the outdoor temperature due to the change in the density of air. Figure 7 shows the power consumption for all cooling and heating tests. Points to the left of the vertical red line are heating tests, and the ones to the right are cooling tests.

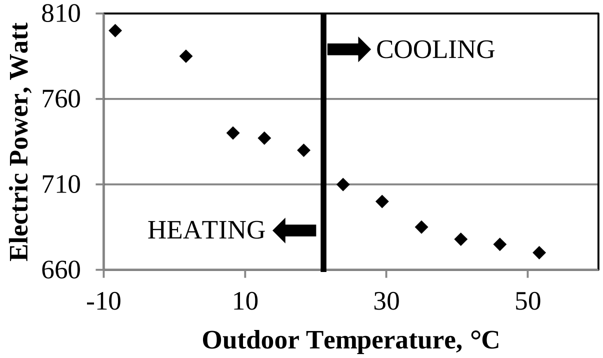

Figure 7. Electric power consumption of the outdoor unit of the GHP in cooling (right of the vertical line) and heating (left of the vertical line.)

Air handler power consumption was 950 watts on high stage and 300 watts on low stage.

5. TECHNICAL AND MARKET BARRIERS

The current residential GHP has some limitations from both overall cost and engine performance and point of view. These shortcomings are:

High initial cost: The current system costs over $14,000. The manufacturing and assembly processes and equipment are not geared for high-volume, repetitive, lowest-cost production. These are the major market barrier for this technology. Most of the off the shelf components will be reduced significantly with quantity mass procurement. However, components like engine, compressor, and exhaust to coolant heat exchanger, and system controllers will require redesign and/or identifying alternate parts. The current engine sub-assembly costs over $4000 or 35% of the total unit cost. This is the major hurdle in achieving commercial viability of the residential GHP. Initial comments from the current engine provider indicated that there is not a significant potential in reducing the engine cost.

Limited engine power output and low thermal efficiency: The current single cylinder IC engine has shown limitation in terms of achieving the desired cooling capacity of 17.6 kW (60,000 Btu/h or 5 RT) at the ARI rating condition. In addition, the thermal efficiency of the IC engine needs improvement from the current low 20%. In order for RGHP to compete with high efficiency current state of the art electric heat pumps, the engine fuel to shaft power conversion efficiency need to be in the range of 28-30%.

Low frequency noise: These sound-generating vibrations derive from the combustion in the cylinder and the corresponding pressure waves in the intake and exhaust systems. They are all keyed to the engine's rotational speed; as the engine speed rises or falls, the pitch goes up or down.

Market acceptance: GHPs in general suffer from low awareness and poor perception. The latter is particularly relevant to the residential GHP. This is due a failed commercialization of a residential GHP in early 2000s. In order for the residential GHP to gain market penetration, there must be greater exposure of the technology to end-users, installers, designers and contractor.

Regulatory issues: the current regulatory landscape is moving towards a treatment of GHP (distributed generation) as either providing solely regulated services (in which case the cost can be rate based) or having to recover all of its costs through the market. A hybrid treatment of GHP that can better capture market and non-market services, such as unbundling, can provide more efficient GHP development. Government support, such as the use of investment tax credits, can help mitigate the riskiness of this technology, improve project economics, and lower deployment barriers. Utilities and end users may also avoid or reduce risk by contracting energy storage services to third party service providers, which then assumes any associated risk. Tying GHP to renewables is another means to promote the product. Moreover, many of the non-technical issues that limit GHP deployment are likely to raise similar barriers to the competing solutions. Thus, to the extent that addressing these issues can make the proposed technology more attractive, it will often improve the economics of these competing technologies. It will require continued engagement with regulators, policy makers, market operators, utilities, and manufacturers to mitigate identified barriers.

Incomplete valuation: better tools are needed to better valuate the full benefits that GHP can provide. This can be addressed through further research and model development, as well as more transparent pricing of energy-system services and control technologies to end users.

6. CONCLUSION

Laboratory performance of residential scale GHP was presented. Though GHP can provide numerous benefits to consumers, there are a number of factors that restrict its deployment. The most significant barrier to deployment is high capital costs. However, a number of other market and regulatory barriers persist, limiting further deployment. The main barriers were also presented.

NOMENCLATURE

cc	cubic centimeters
h	specific enthalpy (kJ/kg)
$\dot{m}$	mass flow rate (kg/s)
p_{ws}	saturation pressure of water vapor in air (Pascal)
rev	revolution
t	dry-bulb temperature (°C)
v	specific volume (m3/kg)
ρ	density (kg/m3)
COP	coefficient of performance
C_p	specific heat under contant pressure (kJ/kg-°K)
GHP	gas engine driven heat pump
HP	horsepower
P	pressure (Pascal)
PC	personal computer
Q	cooling or heating capacity (kW)
RT	refrigeration ton
SHR	sensible heat ratio
T	dry-bulb emperature (°K)
$\dot{V}$	volumetric flow rate (m3/s)
W	humidity ratio

Subscript

r	return air
s	supply air
L	latent
S	sensible
T	total

REFERENCES

ASHRAE 2006. ANSI ASHRAE Standard 41.1-1986 (RA 2006), Standard Method for Temperature Measurement. *Atlanta: American Society of Heating, Refrigeration, and Air Conditioning Engineers, Inc.*

ASME 2004a. ASME Power Test Code 19.2-1987 (Reaffirmed 2004), Instruments and Apparatus, Part 2, Pressure Measurements. *New York: American Society of Mechanical Engineers.*

ASME 2004b. ASME Power Test Code 19.2-2004, Flow Measurement. *New York: American Society of Mechanical Engineers.*

ASHRAE 1989a. ANSI/ASHRAE Standard 41.3-1989, Standard Method for Pressure Measurement. *Atlanta: American Society of Heating, Refrigeration, and Air Conditioning Engineers, Inc.*

American Society of Heating, Refrigerating and Air-Conditioning Engineers, 2005, 2005 ASHRAE Handbook: Fundamentals, *Atlanta, Ga: American Society of Heating Refrigerating and Air-Conditioning.*

Delta Energy & Environment Ltd., David Strong Consulting Ltd., 2014, RHI Evidence Report: Gas Driven Heat Pumps, *Department of Energy and Climate Change, United Kingdom.*

Goetzler, Willian, Zogg, Robert, Young, Jim, Justin, Shmidt, 2012, Energy Savings Potential and RD&D Opportunities for Residential Building HVAC Systems, *Navigant Consulting, Inc. prepared for U.S. Department of Energy, Office of Energy Efficiency and Renewable Energy, Building Technologies Office.*

Mahderekal, Isaac Y., Gaylord, Robert G., Young, Tommis, Hinderliter, Kevin, 2008, Design and Development of a Gas-Engine-Driven Heat Pump, *ASME 2008 2nd International Conference on Energy Sustainability, Volume 1: 609-617.*

Mahderekal, Isaac, Shen, Bo, and Vineyard, Edward A., 2012, System Modeling of Gas Engine Driven Heat Pump, *International Refrigeration and Air Conditioning Conference. Paper 1199.*

Shen, Bo, Mahderekal, Isaac, and Vineyard, Edward A., 2013, System Modeling and Building Energy Simulations of Gas Engine Driven Heat Pump, *HVAC&R Research*

Sohn, Chang W., Franklin H. Holcomb; Dudley J. Sondeno, and James M. Stephens, 2008, Field tested cooling performance of gas engine-driven heat pumps. SL-08-023. *ASHRAE Transactions, Volume 114 (Part 2): pp 232-239.*

U.S. Energy Information Agency, 2015, Annual Energy Outlook 2015 with Projections to 2040, *DOE/EIA-0383(2015)*

ACKNOWLEDGMENTS

This work was sponsored by the U. S. Department of Energy's Building Technologies Office under Contract No. DE-AC05-00OR22725 with UT-Battelle, LLC. We would like to acknowledge Mr. Antonio Bouza the Technology Manager for the HVAC & Appliances for his support. The authors would like to also acknowledge support from ORNL's Neal Durfee, Randal Linkous and Philips Childs, and Gary Rose from IntelliChoice Energy for their assistance.